ELSEVIER

Colloids and Surfaces
A: Physicochemical and Engineering Aspects 187–188 (2001) 469–481

COLLOIDS AND SURFACES A

www.elsevier.nl/locate/colsurfa

Transport properties of porous membranes based on electrospun nanofibers

Phillip Gibson *, Heidi Schreuder-Gibson, Donald Rivin

Materials Science, AMSSB-RSS-MS, US Army Soldier Systems Center, Natick, MA 01760-5020, USA

Abstract

Electrospinning is a process by which high voltages are used to produce an interconnected membrane-like web of small fibers (10–500 nm in diameter). This novel fiber spinning technique provides the capacity to lace together a variety of types of polymers, fibers, and particles to produce ultrathin layers. Of particular interest are electrospun membranes composed of elastomeric fibers, which are under development for several protective clothing applications. The various factors influencing electrospun nonwoven fibrous membrane structure and transport properties are discussed. Performance measurements on experimental electrospun fiber mats compare favorably with transport properties of textiles and membranes currently used in protective clothing systems. Electrospun layers present minimal impedance to moisture vapor diffusion required for evaporative cooling. There may be special considerations in the application of elastomeric membranes for protective clothing. Effects of membrane distortion upon transport behavior of the structure might be significant. Preliminary measurements have found that changes in elastomeric membrane structure under different states of biaxial strain were reflected in measurements of air flow through the membrane. Changes in membrane structure are also evident in environmental scanning electron microscope (SEM) images of the pore/fiber rearrangement as the membrane is stretched. Experimental measurements and theoretical calculations show electrospun fiber mats to be extremely efficient at trapping airborne particles. The high filtration efficiency is a direct result of the submicron-size fibers generated by the electrospinning process. Electrospun nanofiber coatings were applied directly to an open cell polyurethane foam. The air flow resistance and aerosol filtration properties correlate with the electrospun coating add-on weight. Particle penetration through the foam layer, which is normally very high, was eliminated by extremely thin layers of electrospun nanofibers sprayed on to the surface of the foam. Electrospun fiber coatings produce an exceptionally lightweight multifunctional membrane for protective clothing applications, which exhibits high breathability, elasticity, and filtration efficiency.

Keywords: Electrospinning; Electrospun; Porous; Membrane; Fiber

1. Introduction

Electrospinning is a process by which a suspended droplet of polymer solution or melt is charged to high voltage to produce fibers [1–3].

* Corresponding author. Tel.: +1-508-2334273; fax: +1-508-2335521.
E-mail address: phil.gibson@natick.army.mil (P. Gibson).

0927-7757/01/$ - see front matter
PII: S0927-7757(01)00616-1

At a voltage sufficient to overcome surface tension forces, fine jets of liquid shoot out toward a grounded target. The jet is stretched and elongates before it reaches the target, dries and is collected as an interconnected web of small fibers. The technique provides the capacity to lace together a variety of types of polymers and fibers to produce ultrathin layers, which are useful for chemical protective clothing. Depending on the specific polymer being used, a range of fabric properties, such as strength, weight and porosity, can be achieved. Fig. 1 shows that much smaller fiber diameters and increased surface areas are accessible through the electrospinning technique as compared with currently available textile fibers. Fiber sizes of 40 nm and smaller have been reported [4], although we normally produce fibers in the 200–500 nm range in our apparatus. Fig. 2 shows micrographs of typical electrospun fibers.

Electrospinning results in submicrometer size fibers laid down in a layer that has high porosity but very small pore size. For fibers spun from polymer solutions, the presence of residual solvent in the electrospun fibers facilitates bonding of intersecting fibers, creating a strong cohesive porous structure. The nanofibers assemble into a membrane-like structure that exhibits good tensile strength, excellent moisture vapor transport, extremely low air permeability and good aerosol particle protection.

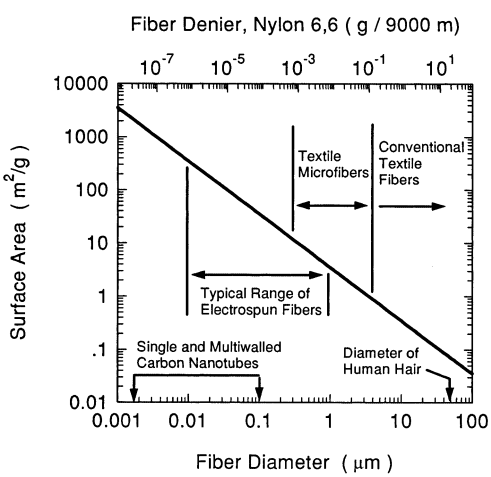

Fig. 1. Electrospun nanofibers have high surface area.

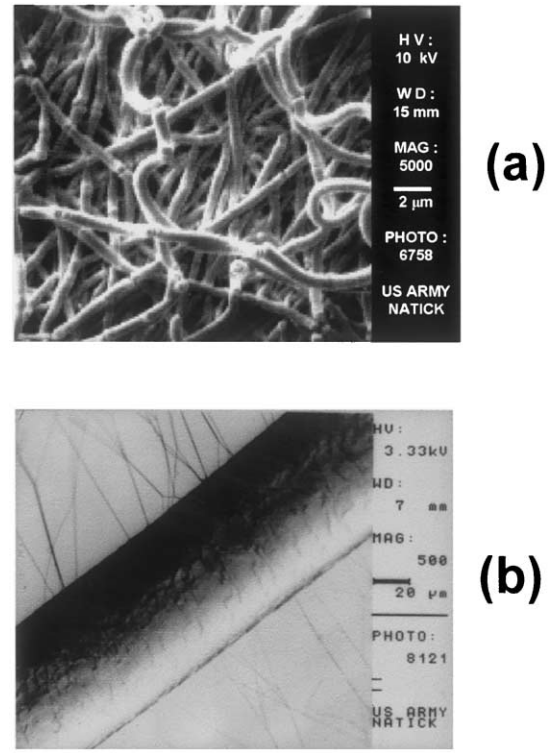

Fig. 2. (a) SEM image of Nylon 6,6 electrospun fiber mat; (b) SEM image of nylon 6,6 nanofibers spun across surface of human hair fiber.

Electrospun nanofiber membranes may be produced over a wide range of porosity values, from nearly nonporous polymer coatings, to very porous and delicate fibrous structures. Our current interest is in consolidated membrane structures with porosities ranging from 30 to 60%. Typical capillary flow liquid expulsion porometry measurements indicate that pore throat diameters range from 0.1 to 0.8 μm in size.

One implication of this type of membrane architecture is that these materials would provide good resistance to the penetration of chemical and biological warfare agents in aerosol form, while still allowing significant water vapor transport to promote evaporative cooling of the body. Electrospun nonwoven fiber mats may be thought of as a microporous material that behaves like a membrane, as opposed to a more porous, air-permeable fabric. Because of the small fiber/pore sizes in these electrospun membranes, the resistance to

convective gas flow is quite large and is comparable to the flow resistance shown by microporous polytetrafluoroethylene (PTFE) membranes, which are often used as a component of protective clothing systems.

Our main interest in electrospun nanofiber membranes has been for chemical/biological protective applications. Recently, we have directly incorporated activated carbon, carbon nanotubes, and submicron enzyme particles into electrospun membranes. Besides chemically protective clothing applications, electrospun nanofibers are under consideration for air and water filtration applications, polymer composite reinforcement, and electrically conductive polymeric networks [5].

A significant advantage of electrospun membranes is that they may be sprayed directly onto three-dimensional (3-D) forms. This is analogous to the electrostatic spray painting technique used for painting metal objects such as car bodies and metal parts. The ability to produce coated objects with a microporous fibrous layer has advantages in terms of eliminating seams, and in the ability to vary the thickness of the nanofiber coating at various locations over the surface of the object. Certain military applications such as boot and glove liners, chemical/biological protective clothing, and flexible gas mask hoods suffer from seam-sealing problems; 3-D net shape electrospinning offers one possible avenue for a solution.

This paper's overall objective is to summarize information related to the transport properties of electrospun membranes both as single layers, and as coatings applied to existing military chemical/biological protective clothing systems. Results are presented for water vapor diffusion and air permeability (important for comfort) and aerosol particle penetration (important for protection from chemical and biological warfare agents).

2. Experimental method

2.1. Water vapor diffusion and gas convection

Water vapor diffusion and gas convection properties of electrospun fiber mats were determined with an automated dynamic moisture permeation cell [5–7]. Gas flows of known temperature and water vapor concentration enter the test cell; by measuring the temperature, water vapor concentration, and flow rates of the gas leaving the cell, one may determine the fluxes of gas and water vapor transported through the test sample. With no pressure difference across the sample, transport of water vapor proceeds by pure diffusion, driven by vapor concentration differences. If a pressure difference across the sample is present, transport of vapor and gas includes convective transport, where the gas flow through the sample carries water vapor with it, which may add to or subtract from the diffusive flux, depending on the direction of the convective gas flow.

Permeability to convective gas flow is given by Darcy's Law [8] such that:

$$k_{\mathrm{D}} = \left(\frac{\mu Q}{A}\right)\left(\frac{\Delta x}{\Delta p}\right) \tag{1}$$

where k_{D} is the permeability constant (m^2), μ the gas viscosity (17.85×10^{-6} kg m^{-1} s for N_2 at 20°C), Q the total volumetric flow rate (m^3 s^{-1}), A the area of test sample (m^2), Δx the thickness (m) and Δp is the pressure drop across sample (N m^{-2} or Pa).

For textiles, although thickness measurements seem simple, they are often problematic, and can be a large source of error if they are incorporated into reported measurements of Darcy permeability. It is preferable to present the pressure-drop/flow rate results in terms of an apparent flow resistance defined as:

$$R_{\mathrm{D}} = \left(\frac{A\Delta p}{\mu Q}\right) \tag{2}$$

where R_{D} is the apparent Darcy flow resistance (m^{-1}).

We define the resistance to mass transfer by diffusion as the simple addition of an intrinsic diffusion resistance due to the sample (R_{i}) and the diffusion resistance of the boundary air layers (R_{bl}):

$$(R_{\mathrm{i}} + R_{\mathrm{bl}}) = \left[\frac{\Delta \bar{C}}{(\dot{m}/A)}\right] \tag{3}$$

where R_{i} is the intrinsic diffusion resistance of sample (s m^{-1}), R_{bl} the diffusion resistance of boundary air layers (s m^{-1}), $\dot{m}$ the mass flux of water vapor across the sample (kg s^{-1}), A the

area of test sample (m^2), $\Delta\bar{C}$ is the log mean water vapor concentration difference between top and bottom nitrogen streams (kg m^{-3}).

The test material's intrinsic diffusion resistance may be obtained by subtracting the apparent boundary layer diffusion resistance [6], but in many cases, it is sufficient to leave the results in the form of a total resistance to water vapor diffusion which includes the boundary layer effects.

2.2. Aerosol filtration

The aerosol particle filtration test system is based on the apparatus described by Park and Rivin [9]. The majority of aerosol particles generated by this system are between 1 and 5 μm. A dilute solution of aqueous potassium iodide is atomized with an ultrasonic nebulizer; the resulting mist of liquid salt solution is diluted with dry nitrogen and flows to a heated drying chamber. The liquid evaporates in the drying chamber to create a solid salt aerosol, which is passed through the filter test material. Aerosol particle size and concentration are monitored by an aerosol analyzer (API Aerosizer, Amherst Instruments, Inc.) which measures the time of flight of individual particles as they pass through two laser beams. The aerosol analyzer is capable of particle size measurement over the range of 0.5–200 μm. Further details of the test system are available in [9,10].

The sample test area clamped in the holder exposed a circular area of 1.34×10^{-3} m^2 to the aerosol stream. The approximate test temperature at the sample holder was 40°C, and the equivalent nitrogen volumetric flow rate at this temperature was 2.1×10^{-5} m^3 s^{-1}. Thus the nominal flow velocity through the sample (u_0) was 0.0157 m s^{-1}. Mean aerosol particle size was 2–3 μm [10].

A useful measure for comparing the filtration performance of different materials is the total amount of aerosols removed from the gas stream. One may also be interested in the relative filtration performance for different particle sizes of aerosols. For this report, we compare performance based on the experimental filtration efficiency given by:

$$E = \frac{n_2 - n_1}{n_2} \quad (4)$$

where n_2 is the aerosol particle concentration upstream, and n_1 is the concentration downstream of the filter test sample. Alternatively, the penetration ratio P may be used, which is defined by $P = 1 - E$.

2.3. Factors affecting selection of test conditions

The filter velocity used for testing the materials is low compared with normal filter test conditions for industrial filters. The difference arises from the fact that the use of clothing materials as aerosol barriers is quite different from porous materials used as filters. Filters are commonly placed in systems, which have a well-defined flow rate or pressure drop across the filter material. In clothing systems, however, the aerosol barrier is incorporated into a clothing system covering the human body, usually with air gaps present between the body and the clothing. An external air flow due to wind or body motion impinges on the clothed human, and some air flows around the body, while some penetrates through the clothing system and into the air gap between the clothing and body, where aerosol deposition on the skin may occur. For a given external air velocity, the amount of air which flows around the body, and the amount which penetrates through the aerosol barrier layer is determined by the air flow resistance (air permeability) of the barrier layer. Materials with a low air flow resistance allow a relatively high flow rate through the fabric, with a correspondingly low pressure drop. Materials with a high air flow resistance allow less flow through the fabric, and have a higher pressure drop across the fabric layer (up to the limit of the stagnation pressure for the particular environmental flow conditions). For a truly valid comparison between aerosol barrier materials which differ in their air permeability properties, it would be desirable to test at a unique volumetric flow rate/filter velocity and pressure drop which corresponds to that produced by a given external air velocity on a typical clothing system.

Some methodologies have been developed for rational aerosol testing of protective clothing ma-

terials which takes these factors into account [11–13]. However, to minimize the number of tests for preliminary characterization efforts, one flow velocity test condition was used for this study. The filter flow velocity (u_0) of 0.0157 m s^{-1} selected for the aerosol test system is a compromise — this flow rate across the porous membranes and most of the electrospun layers results in very high pressure drops that would be unrealistic in any clothing system. Thus, the aerosol test conditions for the materials with a high flow resistance are very much a 'worst case' situation. However, for the materials with a low flow resistance, the flow rates through the fabric would be higher than the relatively low flows and low pressure drops used in the aerosol test system. As will be seen later, the fact that the electrospun layers exhibited high filtration efficiencies compared with common fabric materials, even though the test conditions were relatively unfavorable, indicates the usefulness of these materials for protective clothing applications.

3. Results

3.1. Water vapor diffusion and gas flow properties

The magnitude of the convective flow resistance for two typical electrospun membranes composed of polyacrylonitrile and polybenzimidazole [14] is shown in Fig. 3, and compared with other common fiber-based materials. Fig. 3 shows the gas flow resistance as a function of relative humidity, which is of most importance in the case of a hydrophilic fiber, such as cotton [15].

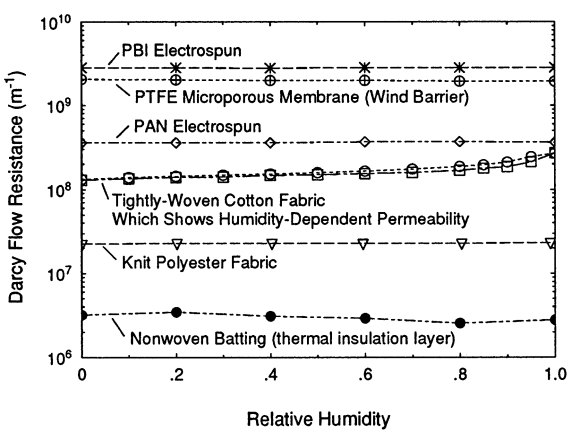

Fig. 3. Microporous membranes and electrospun nonwovens have high convective gas flow resistance.

The convective flow resistance of the electrospun fiber mats is quite large compared with normal clothing materials, yet, as will be shown later, the high resistance to air flow does not impede the diffusion of water vapor through the pore structure of the electrospun nonwoven material. In general, materials with high rates of water vapor diffusion and low air permeability are promising candidates for protective clothing applications.

An interesting complicating factor in the analysis of gas flow through porous materials with such small fiber diameters is that the mean free path of gas molecules becomes comparable to the fiber size [16]. There is gas slip at the fiber surface, and the normal linear dependence of flow rate with pressure drop, valid in low Reynolds number laminar flows, becomes less applicable to the flow field in the electrospun nonwoven pores. It has been estimated that the pressure drop predicted by assuming continuum flow through beds of fibers is reduced by a factor of about 1/3 for a fiber diameter of 0.1 μm [17].

Water vapor transport properties of electrospun nonwovens are excellent and indicate that layers based on electrospun fiber technology will be thin, lightweight, and very 'breathable' with respect to allowing evaporative cooling to take place through the protective clothing system. Water vapor diffusion measurements for the same materials given in Fig. 3 are shown in Fig. 4. The electrospun nonwoven resistance to water vapor diffusion is much lower than the commercially available membrane laminates presented in Fig. 4, which are often said to be highly 'breathable'. Fig. 4 compares the performance of the materials as a function of the 'mean relative humidity', which is useful as an indication of concentration-dependent transport behavior in polymer membranes and membrane laminates [6,7].

Electrospinning also lends itself very easily to spraying a fiber coating directly onto other materials. For example, an extremely thin electrospun

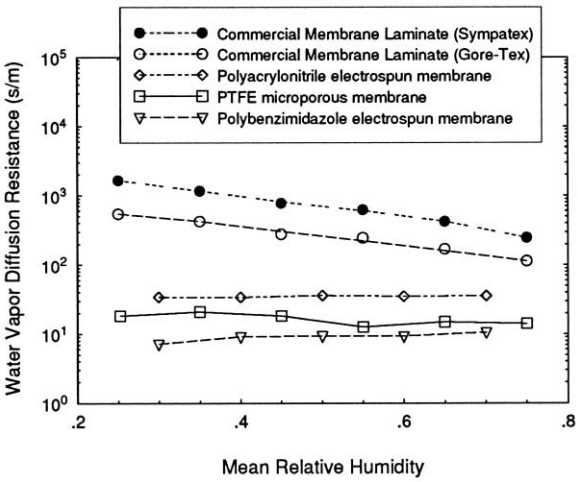

Fig. 4. Electrospun nonwovens have excellent water vapor transport properties.

fiber coating may be sprayed onto the surface of chemical/biological protective garments to improve aerosol particle filtration and capture, or to incorporate additional functionality to the protective garment such as agent-specific enzymes or catalysts. These reactive components would be exposed to reaction conditions in either liquid or vapor phases under varying flow environments.

Water vapor diffusion resistance and air flow resistance properties were determined for an electrospun nonwoven (nylon 6,6) deposited onto an activated-carbon-loaded polyurethane foam, which was an experimental variant of the material used as a chemical protective layer in the US Army Battle Dress Overgarment (BDO). This foam had a nominal thickness of 8.7×10^{-4} m with an areal density of 0.19 kg m^{-2}; the open foam structure results in very little resistance to convective air flow (flow resistance is 3.2×10^{6} m^{-1}). Foam thickness and areal density may vary as much as 10% from the mean value. Scanning electron microscope (SEM) images of the porous carbon-loaded polyurethane foam, and the nylon nanofiber coating on the surface and over the pores of the foam, are shown in Fig. 5.

Seven different electrospun coating add-on levels were produced over the range of 1.6×10^{-4}–1.1×10^{-2} kg m^{-2}. Three other materials were also tested for comparison purposes, (1) the uncoated foam; (2) the uncoated foam tested in combination with a microporous PTFE membrane; (3) the microporous PTFE membrane by itself.

Water vapor diffusion and air flow resistance properties were determined under simultaneous diffusion/convection conditions in the DMPC, as shown in Fig. 6.

Gas enters the DMPC at a relative humidity of 0.90 (90% r.h.) on the top portion of the cell, and 0.0 (0% r.h.) on the bottom of the cell. The automated valves are used to restrict the flow on one or the other sides of the cell. This causes the pressure in one side of the cell to be higher than in the other, producing convective gas flow through air-permeable samples, in addition to the diffusion flux taking place due to the concentration gradients.

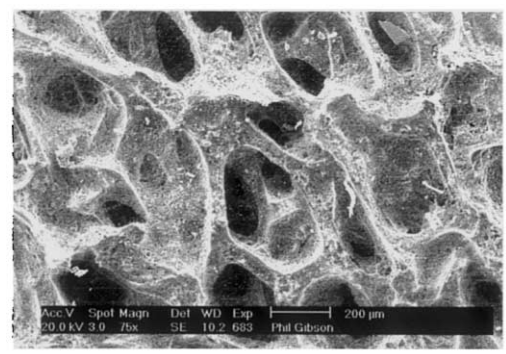

(a) 75x, scale bar is 200 µm

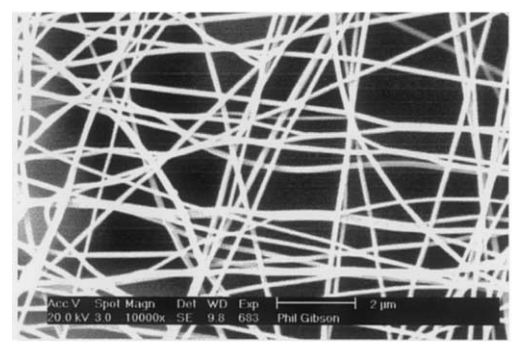

(b) 10,000x, scale bar is 2 µm

Fig. 5. (a) Porous polyurethane foam containing activated carbon; (b) electrospun nylon 6,6 nanofiber coating sprayed onto surface of the foam.

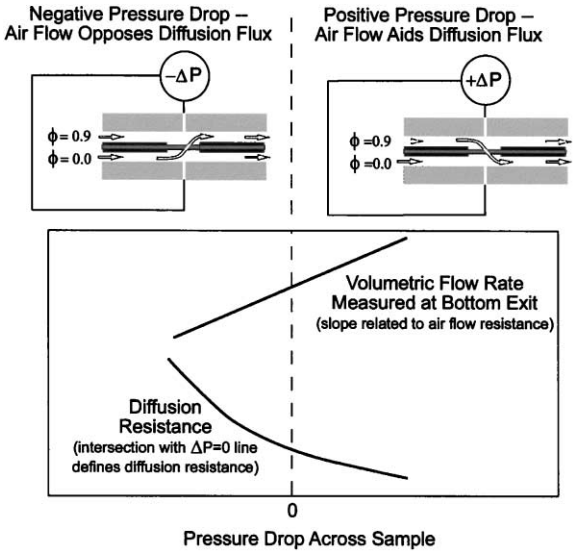

Fig. 6. Convection/diffusion experiment in the DMPC.

Measurements are taken as a function of pressure drop across the sample, where the convective flow and pressure drop are gradually increased in stepwise increments. In addition to the pressure drop, an electronic mass flow meter connected to the lower outlet of the cell is used to record the mass flow rate of gas through the test material. More details on this test method, and correlations with other standard methods, are available in [18,19].

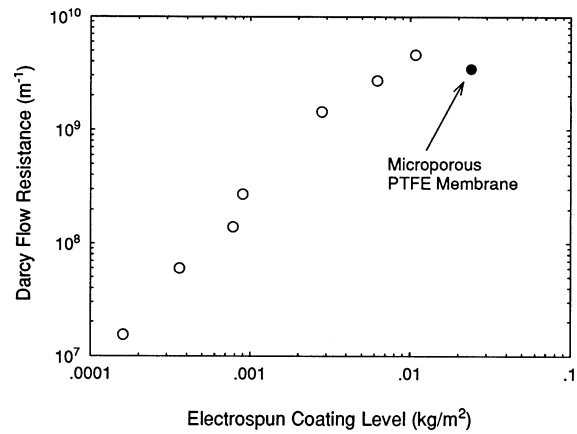

Fig. 8. Convective gas flow resistance related to electrospun coating level.

The plot of convective flow as a function of pressure drop in Fig. 7 shows the expected trends. In this test method, materials with a low slope in Fig. 7 have a high flow resistance; the numerical value of the slope can be converted to a flow resistance as given in Eq. (2).

The electrospun membranes' air flow resistance correlates well with the electrospun layer coating level, as shown in Fig. 8. Fig. 8 also shows the results for the microporous PTFE membrane, which has an areal density comparable to the highest electrospun coating level.

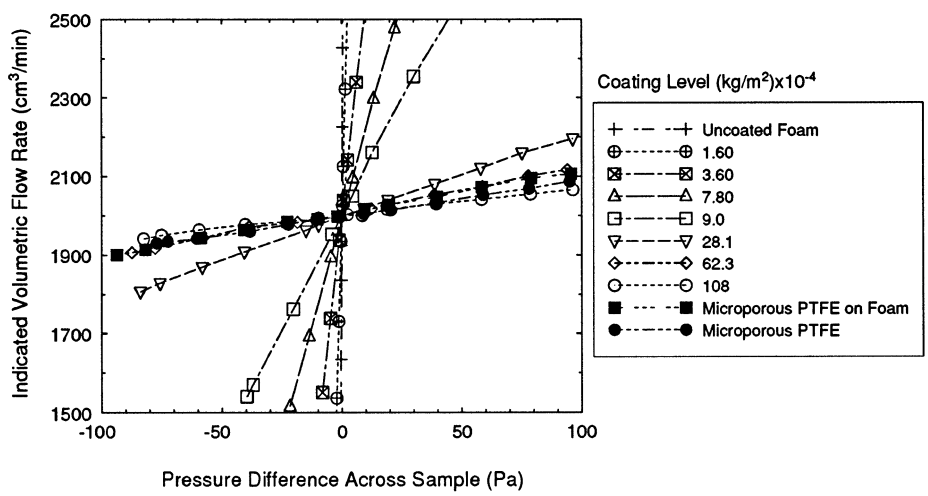

Fig. 7. Convective flow through samples as a function of pressure drop.

The water vapor diffusion resistance as a function of pressure drop (Fig. 9) primarily reflects the different air permeability properties of each coating level. Water vapor diffusion resistance is defined as the intersection of each curve with the point where the pressure difference across the sample is equal to zero. Fig. 9 contains information about both convective and diffusive transport across the test sample. Those materials with higher flow resistances are affected less by the pressure difference across the sample. Fig. 9 includes the boundary layer resistance due to laminar air flow over the sample, which in this case is about 105 s m^{-1}. It is known from previous work [6] that the intrinsic diffusion resistance of the PTFE membrane is 6–8 s m^{-1}. All the electrospun coated foam samples, the foam sample tested in combination with the PTFE membrane, and the uncoated foam sample converge to approximately 200 s m^{-1} at the zero pressure difference point. This translates to an intrinsic diffusion resistance for the samples of approximately 95 s m^{-1} after subtraction of the boundary layer resistance.

The small variations in intrinsic diffusion resistance of the coated and uncoated samples are negligible in the practical sense, since they are within the experimental variation of diffusion resistance caused by the large thickness variations in the foam substrate. It is likely that none of the electrospun layers added more than 10 s m^{-1} to the total diffusion resistance of the foam layer. It is worthwhile to refer to Fig. 4 where the water vapor diffusion resistances of commercial breathable laminates are shown to be much higher (200–1500 s m^{-1}). Other factors in clothing systems, such as stagnant air trapped underneath/between layers, or boundary layer resistances due to air flow over the body surface, also result in water vapor diffusion resistance factors which far outweigh the small contribution of the electrospun membrane layer.

3.2. Aerosol filtration

Aerosol particle filtration properties were determined for an electrospun nonwoven (nylon 6,6) deposited onto an activated-carbon-loaded polyurethane foam. The materials produced were nominally the same as those used for the vapor diffusion and air flow testing presented previously, but the aerosol testing used a separate set of samples.

Eight different electrospun coating add-on levels were produced over the range of 1.2×10^{-4}–1.9×10^{-3} kg m^{-2}. Nominal coating times of 30

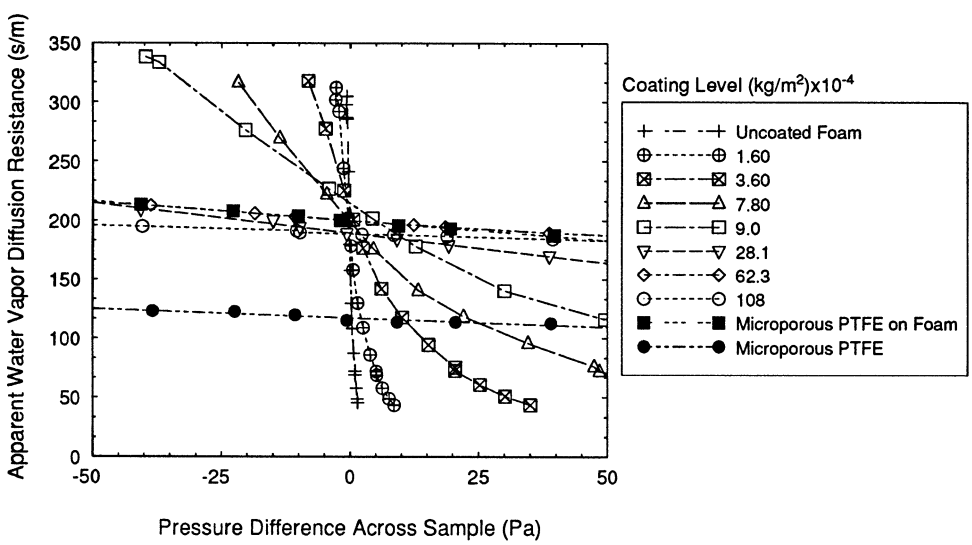

Fig. 9. Water vapor diffusion resistance as a function of pressure drop.

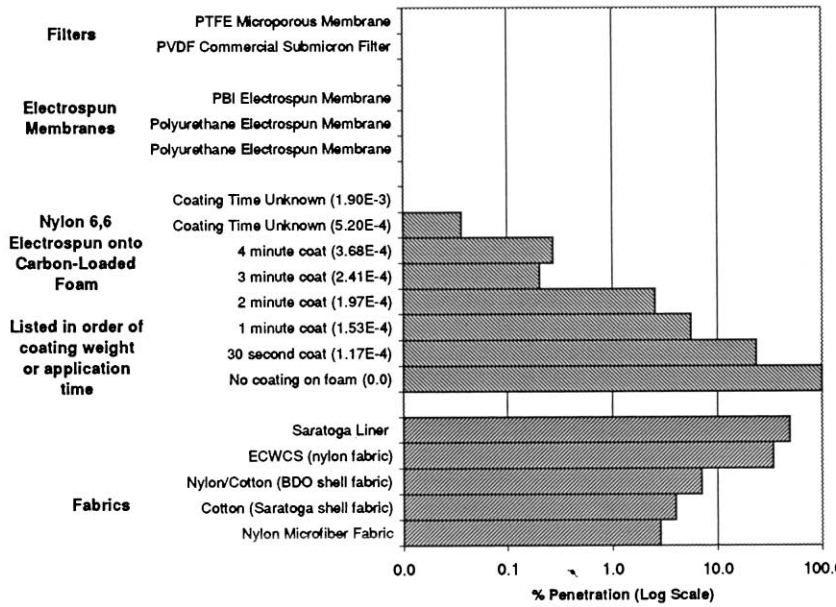

Fig. 10. Comparison of relative aerosol penetration through various porous membranes and textiles. Coating weight listed in parentheses in units of kg m^{-2}.

s, 1, 2, 3 and 4 min were used for the first five coating levels. The last three coating levels were not timed, but were monitored visually to produce increasing coating levels. Unlike the previous set of electrospun coated layers, the coating level was not measured directly. Measuring the coating level is destructive to the sample, since the layer must be peeled or scraped off to measure the weight. Instead, the air flow resistance properties of the electrospun-coated foam samples was measured. The relationship between coating level (kg m^{-2}) and the air flow resistance (1 m^{-1}) given in Fig. 8 was then used to estimate the actual coating level.

Three other classes of materials were also tested for comparison purposes,

1. porous membrane filters consisting of a microporous PTFE membrane and a commercially available polyvinylidene fluoride (PVDF) microporous membrane;
2. stand-alone electrospun membrane layers, one of which was composed of polybenzimidazole fiber, and another two samples spun from polyurethane polymer;
3. five clothing/fabric materials used in military or protective clothing.

The fabric materials included the nylon/cotton fabric used as the outer shell component in the US Army's BDO chemical protective suit. Also tested was the 'Saratoga' chemical protective liner used in the US Marine Corps chemical protective suit, as well as the woven cotton fabric used as the outer shell for this suit. Two tightly-woven nylon fabrics were tested, the nylon fabric used as the outer shell of the US Army's Extreme Cold Weather Clothing System (ECWCS) and a 'microfiber' nylon fabric used as a water-resistant breathable shell in outdoor clothing.

The relative aerosol penetration through the various types of materials is shown in Fig. 10. No aerosol particle penetration was detected for the two microporous membrane filter materials or for the three electrospun membrane samples. For the group of electrospun-coated foam samples, there is a definite relationship between the coating level and the relative aerosol penetration through the coated samples. All the fabric samples show significant aerosol penetration levels, with the nylon microfiber fabric having the best aerosol particle

filtration properties and the Saratoga Liner material the worst filtration properties.

Fig. 11 combines the aerosol filtration properties and the air flow resistance properties of the nylon electrospun-coated polyurethane foam samples. Fig. 11 shows that even the lightest coating of electrospun fibers significantly reduces aerosol penetration through the carbon-loaded polyurethane foam.

Particle size distributions of penetrating particles and SEM micrographs of aerosol particles caught in the electrospun fiber coating are given in [10]. [10] also calculates single fiber overall filter collection efficiencies of electrospun fiber mats according to various standard models [17,20–22].

3.3. Effect of biaxial strain on elastomeric porous nanofiber membranes

In the course of studying microporous membranes for protective clothing systems, we are developing new elastomeric membranes comprised of nonwoven nanofibers. By using the process of electrospinning, highly deformable membrane structures have been made that exhibit strain capacities of over 200% with full elastic recovery. These membranes are soft, flexible, and possess mean pore diameters of < 1 μm.

Measurement of porosity, air flow, and aerosol filtration for highly deformable membranes must be performed carefully on these soft membranes. Furthermore, the ability of these membranes to stretch at flexure points is critical to their performance. These membranes can be laminated to knitted fabrics to impart wind and water resistance to various types of rainwear and sport clothing. However, the permeability of these laminated structures, for example at elbows and knees, would be expected to change upon flexing. There is a need to fully characterize the penetration characteristics of these membranes if they are to be used to protect personnel from biological or aerosol threats.

Electrospun thermoplastic elastomer (TPE) membranes are produced using Pellethane (Dow Chemical) and Estane (B.F. Goodrich) commercial-grade pellets. Electrospinning of these TPEs in solvents such as dimethyl formamide and/or tetrahydrofuran result in a tough elastomeric membrane which looks like a dense nonporous rubber sheet to the naked eye. Samples of these electrospun membranes were stretched in two directions to various strain levels, and tested for water vapor diffusion and air flow properties in the DMPC apparatus [15,23]. Samples under biaxial strain were also examined using an Environmental Scanning Electron Microscope (ESEM)

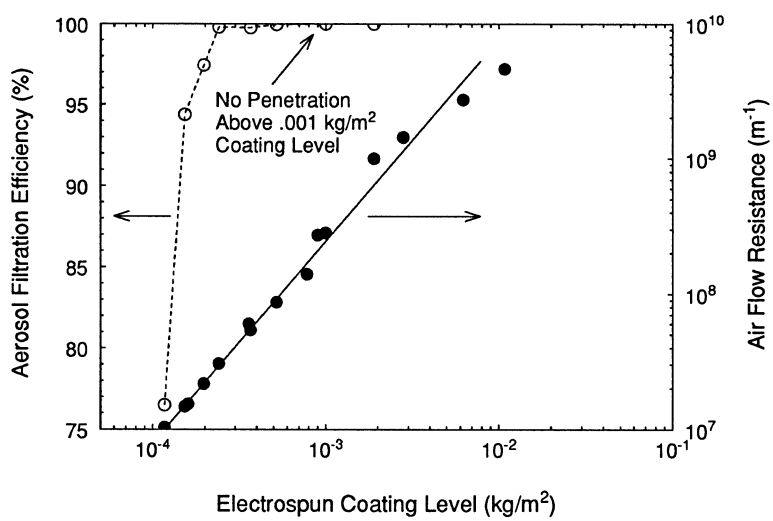

Fig. 11. Aerosol filtration and air flow resistance as function of coating level.

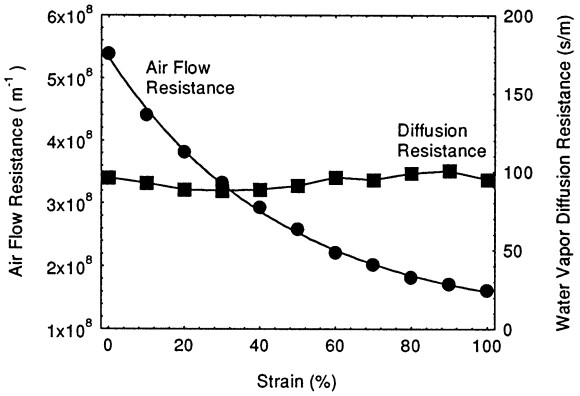

Fig. 12. Effect of strain level on water vapor diffusion resistance and air flow resistance of a porous elastomeric membrane (example shown is pellethane thermoplastic polyurethane).

[24], to observe the changes in pore/fiber structure at different strain levels.

Typical results for an elastomeric nanofiber membrane are shown in Fig. 12.

As might be expected, stretching the membrane uniformly opens up the pores and decreases the measured air flow resistance. However, the change in air flow resistance would still be within the 'windproof' category in terms of the relative properties of protective clothing. It is interesting that the water vapor diffusion properties remain unchanged over the strain levels used for this membrane. This membrane would be categorized as very 'breathable', and the measured resistance to water vapor diffusion is due primarily to the boundary layer flow over the sample surface produced within the DMPC apparatus. Any changes in water vapor diffusion properties caused by pore/fiber rearrangement are insignificant compared with the other effects present in a protective clothing system, such as stagnant air layers between the skin and clothing layers, or the boundary layer present in the external flow over a clothed human.

A visual indication of the physical appearance of an electrospun elastomeric polyurethane membrane at two different strain levels is shown in Fig. 13.

It can be seen that as biaxial strain increases from 0 to 100%, the electrospun fibers begin to straighten and interfiber spacings increase, suggesting a possible increase in porosity. The density of fibers that we see in the image diminishes as strain increases. The fibers in the unstrained elastomeric membrane are much thicker, on average, than they are in the strained membrane. These elastomeric membranes behave much like nonwoven fibrous structures which are widely used in protective clothing, albeit at a much smaller scale of fiber and pore sizes. The advantages inherent in the increased surface area and smaller pore sizes, as well as in the very thin and lightweight nature of membranes based on elastic nanofiber polyurethanes, have many applications in military and civilian protective clothing systems.

4. Conclusions

Performance measurements on experimental electrospun fiber mats compared favorably with transport properties of textiles and membranes

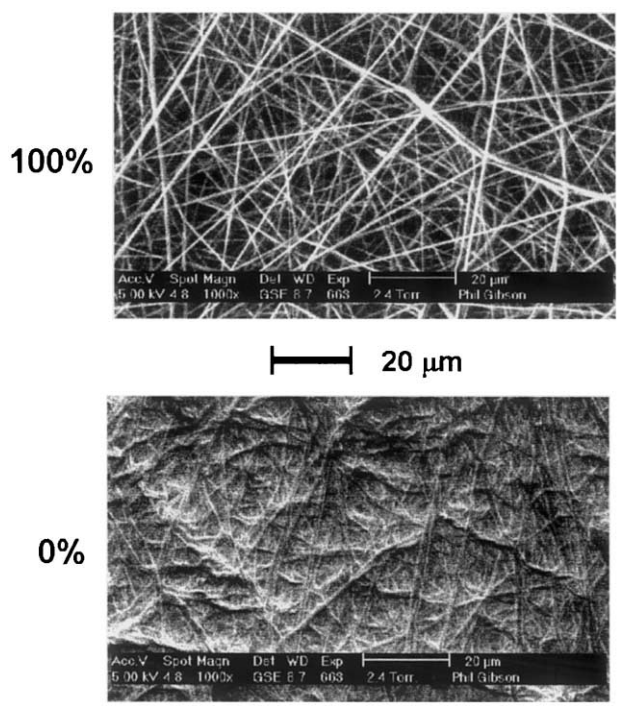

Fig. 13. ESEM images of elastomeric nanofiber membranes under two different levels of biaxial strain.

currently used in protective clothing systems. The electrospun layers presented minimal impedance to moisture vapor diffusion required for evaporative cooling.

Experimental measurements and theoretical calculations showed electrospun fiber mats to be extremely efficient at trapping aerosol particles. The high filtration efficiency is a direct result of the submicron-size fibers generated by the electrospinning process. Because the electrospun fiber diameters are comparable to the mean free path of air molecules, the high pressure drop penalty incurred by small-fiber filter materials which operate in the continuum flow regime is much reduced.

Electrospun nanofiber coatings were applied directly to a polyurethane foam containing activated carbon, which is used as a component in military chemical protective clothing systems. The air flow resistance and aerosol filtration properties correlated with the electrospun coating add-on weight. Aerosol particle penetration through the foam layer, which is normally very high, was eliminated by minuscule levels of nylon electrospun nanofibers sprayed on to the surface of the foam.

Porous elastomeric nanofiber membranes were stretched in biaxial tension to strain levels of 100%. Convective gas flow properties were significantly affected as the interfiber pores opened up. Water vapor diffusion properties remained unchanged within the limits of the test device used for the evaluation. ESEM images of the deformed elastomeric nanofiber membranes confirmed that the elastic fibers were under an increasing state of tension while interfiber pore space increased.

Potential future applications of electrospun layers include direct application of elastomeric membranes to garment systems, eliminating such costly manufacturing steps as laminating and curing. It may be possible to electrospin fibers directly onto 3-D screen forms obtained by 3-D body scanning. Scientists are currently using a laser-based optical digitizing system to record the body surface coordinates of test subjects [25]. This information could be integrated with computer aided design and manufacturing (CAD/CAM) processes to allow electrospun garments to be sprayed onto the digitized form, resulting in custom-fit, seamless clothing.

References

[1] P.K. Baumgarten, Electrostatic spinning of acrylic microfibers, J. Colloid Interf. Sci. 36 (1971) 71.
[2] L. Larronda, R.S. John Manley, Electrostatic fiber spinning from polymer melts. I. Experimental observations on fiber formation and properties, J. Polym. Sci.: Polym. Phys. 19 (1981) 909.
[3] J. Doshi, J. Reneker, D.H. Reneker, Electrospinning process and applications of electrospun fibers, J. Electrostat. 35 (1996) 151.
[4] D. Reneker, I. Chun, Nanometre diameter fibres of polymer, produced by electrospinning, Nanotechnology 7 (1996) 215.
[5] H. Schreuder-Gibson, K. Senecal, M. Sennett, Z. Huang, J. Wen, W. Li, Y. Tu, D. Wang, S. Yang, Z. Ren, C. Sung, Characteristics of electrospun fibers containing carbon nanotubes, in: Proceedings of 197th Electrochemical Society Conference, Toronto, Canada, May 14–19, 2000.
[6] P. Gibson, C. Kendrick, D. Rivin, M. Charmchi, L. Sicuranza, An automated water vapor diffusion test method for fabrics, laminates, and films, J. Coated Fabrics 24 (1995) 322.
[7] P. Gibson, M. Charmchi, The use of volume-averaging techniques to predict temperature transients due to water vapor sorption in hygroscopic porous polymer materials, J. Appl. Polym. Sci. 64 (1997) 493.
[8] F. Dullien, Porous Media-Fluid Transport and Pore Structure, Academic Press, New York, 1979, p. 157.
[9] H.B. Park, D. Rivin, An aerosol challenge test for permeable fabrics, US Army Natick Research, Development and Engineering Center Technical Report, NATICK/TR-92/039L, July, 1992.
[10] P. Gibson, H. Schreuder-Gibson, Aerosol particle filtration, gas flow, and vapor diffusion properties of electrospun nanofiber coatings, NATICK/TR-99/016L, US Army Soldier Systems Center, Natick, MA, February, 1999.
[11] P. Fedele, W. Bergman, R. McCallen, S. Sutton, Hydrodynamically induced aerosol transport through clothing, in: Proceedings of the 1986 Army Science Conference, vol. I, 1986, pp. 279–293.
[12] J. Hanley, P. Fedele, Wind tunnel study of aerosol penetration through protective overgarments, in: Proceedings of the 1987 US Army Chemical Research, Development, and Engineering Center Scientific Conference on Chemical Defense Research, 1988, pp. 444–450.
[13] J. Hanley, D. VanOsdell, P. Fedele, Methodologies for testing permeable chemical protective fabrics and garments against an aerosol threat, in: Proceedings of the 1988 US Army Chemical Research, Development, and Engineering Center Scientific Conference on Chemical Defense Research, 1989, pp. 347–353.

[14] J.S. Kim, D.H. Reneker, Polybenzimidazole nanofiber produced by electrospinning, Polym. Eng. Sci. 39 (5) (1999) 849.
[15] P. Gibson, A.E. Elsaiid, C. Kendrick, D. Rivin, M. Charmchi, A test method to determine the relative humidity dependence of the air permeability of textile materials, J. Testing Eval. 25 (1997) 416.
[16] A.A. Kirsch, I.B. Stechkina, N.A. Fuchs, Gas flow in aerosol filters made of polydisperse ultrafine fibres, Aerosol Sci. 5 (1974) 39.
[17] W. Hinds, Aerosol Technology, Wiley, New York, 1982, pp. 183–184.
[18] P. Gibson, M. Charmchi, Modeling convection/diffusion in porous textiles with inclusion of humidity-dependent air permeability, Int. Commun. Heat Mass Transfer 24 (1997) 709.
[19] P. Gibson, C. Kendrick, D. Rivin, Convection/diffusion test method for porous textiles, Int. J. Clothing Sci. Technol. 12 (2) (2000) 96–113.
[20] R.C. Flagan, Fundamentals of Air Pollution Engineering, Prentice Hall, Englewood, NJ, 1988, pp. 433–455.
[21] K.W. Lee, B.Y.H. Liu, Theoretical study of aerosol filtration by fibrous filters, Aerosol Sci. Technol. 1 (1982) 147.
[22] D. Boulaud, A. Renoux, Stationary and nonstationary filtration of liquid aerosols by fibrous filters, in: K. Spurny (Ed.), Advances in Aerosol Filtration, CRC Press LLC, Boca Raton, FL, 1998, p. 54.
[23] P. Gibson, D. Rivin, C. Kendrick, H. Schreuder-Gibson, Humidity-dependent air permeability of textile materials, Textile Res. J. 69 (5) (1999) 311.
[24] G. Danilatos, Introduction to the ESEM instrument, Microsc. Res. Technol. 25 (1993) 354.
[25] S. Paquette, 3-D scanning in apparel design and human engineering, IEEE Comput. Graphics Applic. 16 (5) (1996) 11.